

## Selecting the Shape of Supported Metal Nanocrystals: Pd Huts, Hexagons, or Pyramids on SrTiO<sub>3</sub>(001)

Fabien Silly and Martin R. Castell

*Department of Materials, University of Oxford, Parks Road, Oxford OX1 3PH, United Kingdom*

(Received 16 August 2004; published 3 February 2005)

Increasing interest in oxide supported nanoparticle science and technology is stimulating research into controlling nanocrystal shape. Pd forms nanocrystals on the surface of SrTiO<sub>3</sub>(001), and depending on the crystallographic interface of the Pd with the substrate three shapes can be created: truncated pyramids, huts, and hexagonal shaped disks. Scanning tunneling microscopy reveals that the nanocrystal shapes are determined by the substrate reconstruction and the substrate temperature during deposition. A thermodynamic model is used to show that the pyramids and huts are stable structures, and that the hexagons are trapped in a metastable state.

DOI: 10.1103/PhysRevLett.94.046103

PACS numbers: 68.47.Jn, 68.37.Ef, 75.70.Kw

Metallic nanocrystals and clusters on oxide supports are in widespread use for heterogeneous catalysis and gas sensing. The size and shape of the nanocrystals are important factors that determine physical and chemical properties such as luminescence, conductivity, and catalytic activity [1–5]. Improvements in current processes and the development of new devices depend in part on our ability to accurately control nanocrystal morphology. Extensive studies have been undertaken in the metal-oxide interface to monitor the growth of small islands [6,7], but until now it has not been possible to select their shape. In this Letter we describe investigations of Pd nanocrystals on SrTiO<sub>3</sub>(001) substrates and show that depending on their interface crystallography three types of structure can be created: truncated pyramids, huts, and hexagonal shaped disks.

Interest in the SrTiO<sub>3</sub> surface has emerged from its widespread use as a substrate for thin film growth and its electronic properties [8]. SrTiO<sub>3</sub> crystallizes into the cubic perovskite structure with a 3.905 Å lattice parameter. In its pure form it has a 3.2 eV band gap which would make it unsuitable for imaging in the scanning tunneling microscope (STM). To overcome this problem, we use crystals doped with 0.5% (molar) Nb. The crystals were epipolished (001) and supplied by PI-KEM, Surrey, U.K.

Pd is widely used in supported small particle form for hydrogenation reactions in heterogeneous catalysis. In its crystalline state Pd adopts the face centered cubic structure with a lattice parameter of 3.890 Å. The lattice mismatch between SrTiO<sub>3</sub> and Pd is therefore only 0.4% so that one might expect an epitaxial relationship for Pd grown on SrTiO<sub>3</sub> surfaces [9]. We deposited Pd from an *e*-beam evaporator (Oxford Applied Research EGN4) using 99.95% pure Pd rods supplied by Goodfellow, U.K. Our STM is manufactured by JEOL (JSTM 4500s) and operates in UHV (10<sup>-8</sup> Pa). We used etched W tips to image the samples at room temperature with a bias voltage applied to the sample. SrTiO<sub>3</sub>(001)-(2 × 1) reconstructed surfaces were prepared by chemically etching the crystals in a

buffered NH<sub>4</sub>F-HF solution and subsequently annealing in UHV at 800 °C for 30 min. Surfaces with a *c*(4 × 2) reconstruction were obtained by Ar<sup>+</sup> sputtering, typically at 500 eV for 10 min, followed by a 900 °C anneal for 30 min. A detailed account of surface preparation and characterization is described in Ref. [10].

Figure 1 shows the topography of the SrTiO<sub>3</sub>(001)-(2 × 1) surface following room temperature deposition of Pd and a subsequent 45 min anneal at 650 °C. Around 300 Pd clusters are visible on the 140 × 140 nm<sup>2</sup> image of

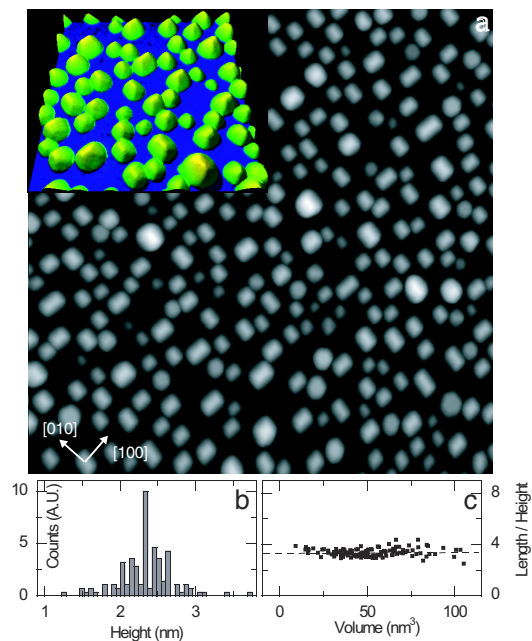


FIG. 1 (color online). Pd deposition onto a room temperature (2 × 1) substrate followed by a 650 °C anneal gives rise to hut clusters as shown in the STM image (140 × 140 nm<sup>2</sup>;  $V_s = +0.8$  V,  $I_s = 0.3$  nA) in (a). The inset shows a 3D rendering highlighting the hut shapes. In (b) a histogram shows the distribution of hut heights. (c) The ratio of hut length to height is constant as a function of cluster volume.

which more than 99% have the shape of the roof of huts as shown in detail in the inset. Figure 1(c) shows the hut length ( $\ell$ ) to height ( $h$ ) ratio as a function of volume. The ratio remains constant with volume where  $\ell/h = 3.48 \pm 0.31$  and the error denotes the standard deviation. This result implies that the huts are at their equilibrium shape. Detailed measurement of the nanocrystal facet angles with respect to the substrate show that the end facets are inclined at  $46.4^\circ \pm 2.7^\circ$  and the side facets at  $36.9^\circ \pm 2.0^\circ$ . The hut heights are quantized by steps of  $1.5 \text{ \AA}$ , close to the  $1.38 \text{ \AA}$  (011) interplanar spacing of Pd [Fig. 1(b)]. The alignment of the rectangular based huts are along the  $\langle 100 \rangle$  directions of the substrate. This indicates that the huts have an (011) interface with (001) end facets and (111) side facets. The interfacial crystallography for the huts is therefore  $(011)_{\text{Pd}} \parallel (001)_{\text{SrTiO}_3}$ ,  $[110]_{\text{Pd}} \parallel [100]_{\text{SrTiO}_3}$ , and hence the Pd huts are related to the  $\text{SrTiO}_3(001)$  substrate via coincidence epitaxy.

The topography of the  $\text{SrTiO}_3(001)-(4 \times 2)$  surface following room temperature deposition of Pd and a subsequent 45 min anneal at  $650^\circ\text{C}$  is shown in Fig. 2. Around 550 clusters can be seen on this  $140 \times 140 \text{ nm}^2$  image of which more than 99% have the shape of hexagonal disks as shown in detail in the inset. The distinct height quantization [Fig. 2(b)] of  $2.2 \text{ \AA}$  corresponds to the Pd (111)

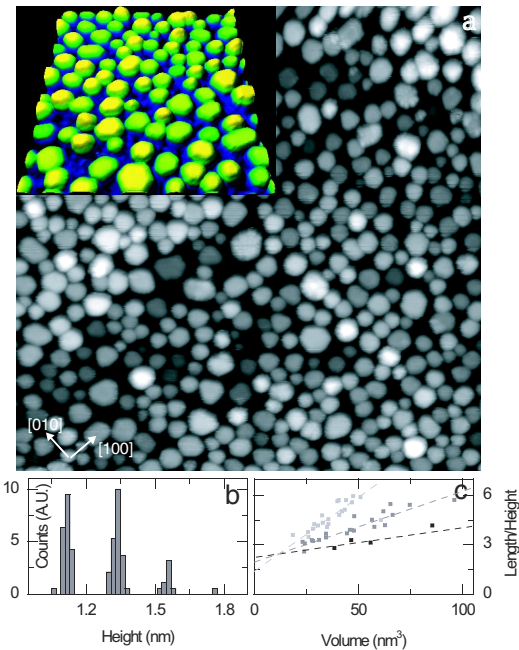


FIG. 2 (color online). Hexagonal nanocrystals are formed following Pd deposition onto a room temperature  $c(4 \times 2)$  substrate followed by a  $650^\circ\text{C}$  anneal as shown in the STM image ( $140 \times 140 \text{ nm}^2$ ;  $V_s = +0.8 \text{ V}$ ,  $I_s = 0.3 \text{ nA}$ ) in (a). The inset shows a 3D rendering highlighting the hexagonal shapes. In (b) a histogram shows the distribution of hexagon heights with three distinct peaks. (c) shows that the ratio of hut length to height increases as a function of cluster volume where light gray, gray, and black correspond to cluster heights of  $11.2$ ,  $13.4$ , and  $15.6 \text{ \AA}$ , respectively.

interplanar spacing ( $2.25 \text{ \AA}$ ) indicating that the top surface is a (111) plane. The top of the hexagons is parallel to the substrate, and its shape is that of a truncated triangle which corresponds to a nanocrystal with a (111) top facet, three (111) side facets, and three (001) side facets. Hence the interface is  $(111)_{\text{Pd}} \parallel (111)_{\text{Pd}} \parallel (001)_{\text{SrTiO}_3}$ ,  $[110]_{\text{Pd}} \parallel [110]_{\text{SrTiO}_3}$ , giving rise to coincidence epitaxy. Figure 2(c) shows the length to height ratio as a function of volume for the three predominant heights. The length in this instance is the width across the top of the hexagon from the middle of one (001) side facet to the middle of the opposite (111) side facet. In contrast to the hut data, the  $\ell/h$  ratio is not constant but increases with cluster volume, indicating that these nanocrystals are not in their equilibrium shapes. Hexagons appear to grow by increasing their width rather than their height. We can find the equilibrium ratio at the intersection of the lines at  $\ell/h = 2.50 \pm 0.33$ . This ratio is also found for isolated hexagons grown at higher temperatures.

If we deposit Pd on a  $c(4 \times 2)$  substrate heated to  $460^\circ\text{C}$  and then carry out the same 45 min anneal at  $650^\circ\text{C}$  as before, a very different crystal shape is observed (Fig. 3). Around 140 Pd nanocrystals can be seen in the  $140 \times 140 \text{ nm}^2$  image of which more than 96% have the shape of a truncated pyramid. A number of flatter hexagons can also be seen. The side facets of the nanocrystals were measured at an angle of  $53.6^\circ \pm 2.5^\circ$  with respect to the substrate. The pyramid heights are quantized by steps of

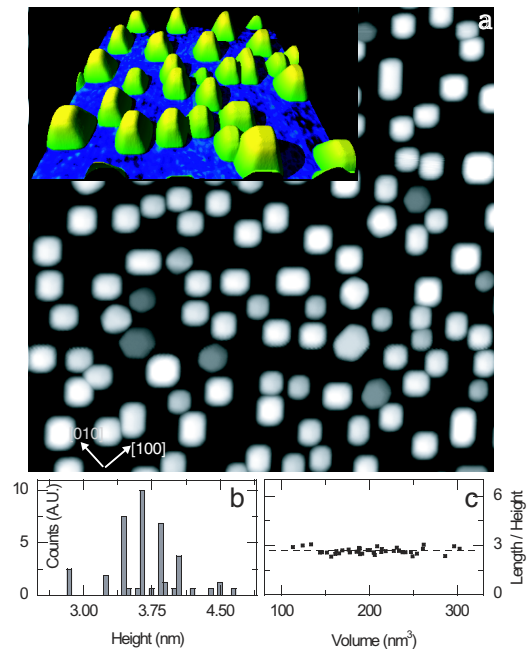


FIG. 3 (color online). Pd deposition onto a  $460^\circ\text{C}$   $c(4 \times 2)$  substrate followed by a  $650^\circ\text{C}$  anneal gives rise to truncated pyramid shaped nanocrystals as shown in the STM image ( $140 \times 140 \text{ nm}^2$ ;  $V_s = +0.8 \text{ V}$ ,  $I_s = 0.3 \text{ nA}$ ) in (a) and the 3D rendered inset. The island height histogram is shown in (b), and the constant height to length ratio is shown in (c).

2.0 Å, close to the 1.95 Å (001) interplanar spacing of Pd [Fig. 3(b)]. The tops and bases of the equilibrium crystals are square. This indicates that the pyramids have four (111) side facets and an (001) top facet as well as an (001) interface, which allows cube on cube commensurate epitaxy with the SrTiO<sub>3</sub>(001) substrate and near perfect lattice matching. The interface crystallography is therefore (001)<sub>Pd</sub> ∥ (001)<sub>SrTiO<sub>3</sub></sub>, [100]<sub>Pd</sub> ∥ [100]<sub>SrTiO<sub>3</sub></sub>. The ratio of the length of the basal square to the height of the truncated pyramids as a function of volume is shown in Fig. 3(c). The constant ratio of  $\ell/h = 2.61 \pm 0.18$  implies that these nanocrystals have reached their equilibrium shape. In this analysis we have not included the pyramids where the basal plane is not square.

Our experimental results above show that Pd can form three distinct nanocrystal shapes on SrTiO<sub>3</sub>(001) depending on the surface reconstruction and the substrate temperature during deposition. As a guide to the eye, we have shown in Figs. 4(d)–4(f) how the Wulff shape can be cut to produce our three supported nanocrystal shapes. The equilibrium shape of a Pd crystal on a SrTiO<sub>3</sub>(001) substrate is determined by the surface energies of the Pd crystal facets ( $\gamma_{hkl}$ ), the interface energy between the Pd crystal and the substrate ( $\gamma_i$ ), and the surface energy of the substrate ( $\gamma_{\text{STO}}$ ). In our case only {111} and {001} facets are seen on the nanocrystals and therefore the change in surface and interface energy between a bare substrate and one supporting a crystal is  $E = \gamma_{001}A_{001} + \gamma_{111}A_{111} + \gamma^*A_i$ , where  $A_{001}$  and  $A_{111}$  are the Pd facet areas,  $A_i$  is the interface area, and  $\gamma^*$  is defined as  $\gamma_i - \gamma_{\text{STO}}$  [11]. For a supported crystal of a given volume to find its equilibrium shape  $E$  will be at a minimum. Using the modified Wulff construction [11] or by minimizing  $E$  analytically results in the following equations for  $\gamma^*$  for each nanocrystal shape as a function of

$\gamma_{001}$ ,  $\gamma_{111}$ , and the length to height ratio:

$$\gamma_{\text{Hut}}^* = \frac{\sqrt{3}\frac{\ell}{h}\gamma_{111} - 4\gamma_{001}}{2\sqrt{2} - \sqrt{2}\frac{\ell}{h}}, \quad (1)$$

$$\gamma_{\text{Hexa}}^* = \sqrt{\frac{3h}{2\ell}}\gamma_{001} - \gamma_{111}, \quad \gamma_{\text{Pyr}}^* = \frac{\frac{\ell}{h}\gamma_{001} - \sqrt{6}\gamma_{111}}{\sqrt{2} - \frac{\ell}{h}}.$$

In these equations we can substitute the  $\ell/h$  ratios from our experimentally determined values, and use the theoretically calculated Pd surface energies of Methfessel *et al.* [12] ( $\gamma_{001} = 1.86 \text{ J/m}^2$ ,  $\gamma_{111} = 1.64 \text{ J/m}^2$ ) which results in  $\gamma_{\text{Hut}}^* = (-1.17 \pm 0.18) \text{ J/m}^2$ ,  $\gamma_{\text{Hexa}}^* = (-0.73 \pm 0.12) \text{ J/m}^2$ , and  $\gamma_{\text{Pyr}}^* = (-0.70 \pm 0.16) \text{ J/m}^2$ .

The energy  $E$  associated with each nanocrystal depends on its shape and volume and can be written as  $E = \alpha_{\text{shape}}V^{2/3}$  where for the three equilibrium nanocrystal shapes

$$\alpha_{\text{Hut}} = 3^{2/3}(\sqrt{6}\gamma_{111} + 2\gamma^*) \times \left( \frac{6\gamma_{001} - \sqrt{3}\gamma_{111} + 2\sqrt{2}\gamma^*}{2\sqrt{6}\gamma_{111} + 4\gamma^*} \right)^{1/3}, \quad (2)$$

$$\alpha_{\text{Hexa}} = \frac{3}{2}\{(\gamma_{111} + \gamma^*)[72\gamma_{001}\gamma_{111} - 12\sqrt{3}\gamma_{001}^2 + \sqrt{3}(\gamma^{*2} + 8\gamma_{111}\gamma^* - 17\gamma_{111}^2)]\}^{1/3}, \quad (3)$$

$$\alpha_{\text{Pyr}} = 18^{1/3}(\sqrt{3}\gamma_{111} + \gamma^*) \left( 1 + \frac{(\gamma_{001} - \sqrt{3}\gamma_{111})^3}{(\sqrt{3}\gamma_{111} + \gamma^*)^3} \right)^{1/3}. \quad (4)$$

Plotting  $\alpha_{\text{shape}}$  as a function of  $\gamma^*$  [Fig. 4(c)] shows that the lowest energy shape depends on the value of  $\gamma^*$ . Comparing these results with our observations we find

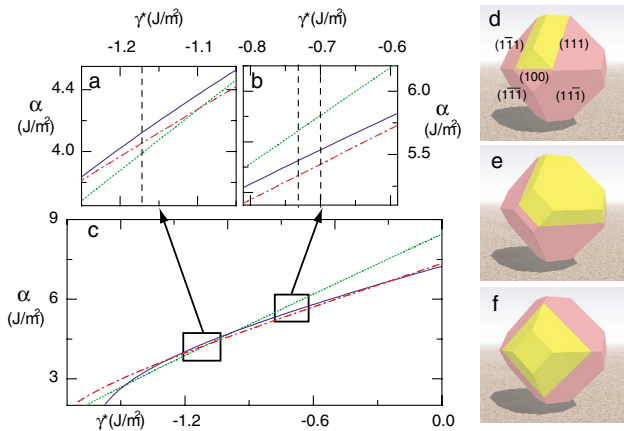


FIG. 4 (color online). Calculated evolution of  $\alpha$  [Eqs. (2)–(4)] with  $\gamma^*$ .  $\alpha_{\text{Hexa}}$  is represented by solid blue line,  $\alpha_{\text{Hut}}$  by dotted green line, and  $\alpha_{\text{Pyr}}$  by dashed red line. (a),(b) Close-up views of the regions of interest in (c). The truncated octahedron crystal habit or Wulff shape of Pd can be cut to produce hut (d), hexagon (e), and truncated pyramid (f) shapes.

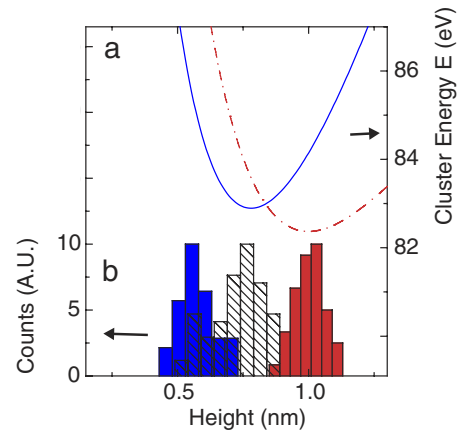


FIG. 5 (color online). (a) Surface energy variation of hexagon (solid blue line) and pyramid (dashed red line) nanocrystals as a function of their height  $h$  at constant volume. (b) The experimental histograms of normalized height of hexagons nucleated at room temperature (blue), hexagons nucleated at 460 °C (hatched) and pyramids (red) are aligned for comparison.

that the experimentally determined  $\gamma^*$  values for the huts and pyramids agree with the correct stability regimes [Figs. 4(a) and 4(b)]; i.e., for  $\gamma_{\text{Hut}}^* = -1.17 \text{ J/m}^2$  the shape with the lowest energy is the hut shape [dotted green line in Fig. 4(a)], and for  $\gamma_{\text{Pyr}}^* = -0.70 \text{ J/m}^2$  the shape with the lowest energy is the truncated pyramid [dashed red line in Fig. 4(b)]. However, our  $\gamma^*$  value for the hexagons indicates that it is in the regime where pyramids are most stable (for  $\gamma_{\text{Hexa}}^* = -0.73 \text{ J/m}^2$  the lowest energy shape is a pyramid [dashed red curve] rather than a hexagon [solid blue curve]). We now look to nonequilibrium effects to explain this discrepancy.

Figure 5(a) shows the hexagon and pyramid nanocrystal energies as a function of height with fixed volume and setting  $\gamma_{\text{Hexa}}^* = -0.73 \text{ J/m}^2$  and  $\gamma_{\text{Pyr}}^* = -0.70 \text{ J/m}^2$  as derived from our experimental data. The fixed volume has been chosen so that  $h = 1 \text{ nm}$  for the pyramid energy minimum, i.e., its equilibrium shape. This plot shows that when Pd grows on a  $c(4 \times 2)$  surface there are two energy minima,  $h = 0.78 \text{ nm}$  (hexagonal shape) and  $h = 1 \text{ nm}$  (pyramid shape). A pyramid cluster that is constrained to be shallower than  $0.83h$  of its equilibrium height [the value where the curves intersect in Fig. 5(a)] has an energy which exceeds that of a hexagonal cluster of the same volume. Therefore, a cluster growing on the  $c(4 \times 2)$  surface that has a height constraint will nucleate and grow as a hexagon even though this is only a metastable state. If no height constraint is imposed, then a pyramid shape will evolve. Once a metastable hexagonal shape has been adopted, there is an energy barrier to reaching the global minimum of a pyramid shape. This explains why we do not observe hexagon to pyramid shape transitions although the pyramids have a lower energy for the same volume. This stands in contrast to strained Ge on Si growth where shape transitions are seen [13,14]. In our experiments we have shown that hexagons are created when the substrate temperature during deposition is low, i.e., when there is little thermal energy for the adsorbed Pd atoms to diffuse. Surface diffusion is a lower energy process than diffusion over a step edge, so that low substrate temperatures during deposition will limit the rate of the growth in height of the nanocrystals, but not in their width. This is the height constraint that gives rise to hexagonal nanocrystal nucleation. In Fig. 5(b), the experimental histograms of normalized height of the clusters show that hexagons that are created during room temperature deposition are flatter than their equilibrium shape due to the energetic barrier of atoms attaching at the side of the crystal to diffuse to the top, whereas hexagons that sometimes nucleate at  $460 \text{ }^\circ\text{C}$  all shift toward the equilibrium shape. More sophisticated modeling of the nanocrystal growth mechanisms needs to take into account kinetic effects, for example, Carter *et al.* [15].

Until now we have restricted our discussion to nanocrystal energies as a function of  $\gamma^*$  (interface energy – substrate surface energy). Experimentally we determined

$\gamma_{\text{Hut}}^* = -1.17 \text{ J/m}^2$ ,  $\gamma_{\text{Hexa}}^* = -0.73 \text{ J/m}^2$ , and  $\gamma_{\text{Pyr}}^* = -0.70 \text{ J/m}^2$ . Given that the hexagons and pyramids are created on the same  $c(4 \times 2)$  reconstructed surface, we can state that the interface energy for the hexagons and pyramids are very close. This may be surprising because the pyramid (001) interface lattice matches to within 0.4% of the substrate, and we have cube on cube epitaxy which should result in a low interface energy. Conversely, the hexagons which have a (111) interface, can lattice match along only one of their three edge directions and have as a result far fewer coincidence sites. Presumably the energetics of the lattice mismatch for the hexagons is compensated by the close packed nature of their (111) interface plane. The huts appear only on a  $(2 \times 1)$  reconstructed surface, and therefore it is not possible to compare the interface energy of the huts with the other shapes. However, the interface energy for the huts is bound to be greater than for the pyramids because epitaxial matching of the Pd (011) interface is achieved in only one  $\langle 001 \rangle$  direction. The low value of  $\gamma^* = -1.17 \text{ J/m}^2$  for the huts is therefore almost certainly a result of a much higher  $(2 \times 1)$  surface energy compared with the  $c(4 \times 2)$  surface energy.

In summary, we have investigated the size and shape distribution of Pd nanocrystals on a  $\text{SrTiO}_3(001)$  support. Our results show that we can select the crystallographic interface of the Pd nanocrystals through modification of the surface reconstruction and substrate temperature during deposition which gives rise to three distinct nanocrystal shapes: huts, hexagons, and pyramids. A thermodynamic model explains the observed results.

The authors thank the Royal Society and DSTL for funding and Chris Spencer (JEOL U.K.) for valuable technical support. We are also grateful to Andrew Powell and Marta Martin for helpful discussions.

- 
- [1] V. Johaneck *et al.*, Science **304**, 1639 (2004).
  - [2] M. Valden, X. Lai, and D. W. Goodman, Science **281**, 1647 (1998).
  - [3] P. L. Hansen *et al.*, Science **295**, 2053 (2002).
  - [4] A. P. Alivisatos, Science **271**, 933 (1996).
  - [5] C. M. Lieber, Solid State Commun. **107**, 607 (1998).
  - [6] G. Renaud *et al.*, Science **300**, 1416 (2003).
  - [7] A. Kolmakov and D. W. Goodman, Chem. Rec. **2**, 446 (2002).
  - [8] D. A. Muller *et al.*, Nature (London) **430**, 657 (2004).
  - [9] T. Wagner, G. Richter, and M. Rühle, J. Appl. Phys. **89**, 2606 (2001).
  - [10] M. R. Castell, Surf. Sci. **505**, 1 (2002).
  - [11] W. L. Winterbottom, Acta Metall. **15**, 303 (1967).
  - [12] M. Methfessel, D. Hennig, and M. Scheffler, Phys. Rev. B **46**, 4816 (1992).
  - [13] G. Medeiros-Ribeiro *et al.*, Science **279**, 353 (1998).
  - [14] F. M. Ross, J. Tersoff, and R. M. Tromp, Phys. Rev. Lett. **80**, 984 (1998).
  - [15] W. C. Carter *et al.*, Acta Metall. Mater. **43**, 4309 (1995).